

# $\mu$ SYNTHESIS OF FLEXIBLE ROTOR MAGNETIC BEARING SYSTEMS

*Kenzo Nonami and Takayuki Ito*

*Chiba University, 1-33 Yayoi-cho, Inage-ku, Chiba 263 Japan*

## ABSTRACT

This paper is described about the research work with simulations and experiments concerned with  $\mu$  synthesis for flexible rotor magnetic bearing system with five-axis-control system of actual test rig. After modelling with the full order system for the flexible rotor system using finite element method, we obtained the reduced order model in modal domain. In this case, every flexible mode in high frequencies was truncated. And we tried to design  $\mu$  synthesis for the reduced order model like rigid rotor.

After choosing the appropriate weighting functions depending on frequency, we designed the  $\mu$  control system using  $\mu$ -toolbox in MATLAB. We tried the simulations of control system for the flexible rotor magnetic bearing system with five-axis-control system and obtained good performances on simulations. Next, we carried out experiments to verify the robustness based on robust control theory for the actual test rig in cases of levitations and rotations. Comparing the control system obtained by the second D-K iteration with the control system before D-K iteration like benchmark test on same conditions, we confirmed that the  $\mu$  control system has excellent performances for robust performances with drastical parameter variations in this test rig.

## 1. INTRODUCTION

Rotor is non-contact supported by electromagnetic forces in magnetic bearings. Therefore, magnetic bearings are used in high speed rotating machinery with many advantages. The advantages of magnetic bearings applied to support a rotor system are its contactless nature, the capability of high speed rotation and active vibration control. So it is necessary to use an asymptotically stable and robust controller for magnetic bearing to support rotor systems. Now the most controllers

designed have been developed by using PID strategy. However, it is not easy to satisfy the robust performance of control systems using PID control law. Of course, modern control theory for multi-input and multi-output(MIMO) system can be applied to magnetic bearing system as advanced control. However, modern control theory also cannot treat with uncertainty which is induced in a mathematical model to design its control system. So, robust control theory is attracted attention for control system design of magnetic bearings these days.

At the present time, there are many robust control theory. In particular, it is well known that  $H^\infty$  control theory[1] and  $\mu$  synthesis[2] are very powerful robust control theory as linear control, and VSS which is variable structure system is also powerful robust control[3] as nonlinear control.  $H^\infty$  control theory includes the advantages of classical control and modern control, and is very systematic as loop shaping theory. However, it is called that  $H^\infty$  control applied to actual system has not always good performances and sometimes very conservative performances. Moreover, it is pointed out that control performances go down in parameter variations in  $H^\infty$  control system. This is caused by maximum singular value. Doyle proposed the structured singular value in addition to maximum singular value to improve control performances[4]. This idea is established as  $\mu$  synthesis theory now[5].

$\mu$  synthesis can treat with robust performances including robust stabilities and nominal performances. Therefore, it is called that  $\mu$  synthesis is an inclusive robust control theory, in particular, is very powerful for parameter variations. So, it is generally known that  $\mu$  synthesis is superior to  $H^\infty$  control theory. Unfortunately, we don't have analytical approach like  $H^\infty$  control theory to design the controller of  $\mu$  synthesis yet. Designing the control system, we have to use the numerical approach which is called the D-K iteration.

This is the biggest problem for  $\mu$  synthesis. So, if we try to design the robust control system using  $\mu$  synthesis, nobody knows whether we can get to good compensator or not after D-K iterations. It is called that it depends on control object, control specification, generalized plant and frequency weighting functions.

In this paper,  $\mu$  synthesis has been applied to the flexible rotor-magnetic bearing system to verify a robust performance comparing with  $H^\infty$  control. In particular, we have obtained excellent data by D-K iteration. Namely, it is found that the static stiffness of magnetic bearing goes up by the first D-K, the second D-K. Though the limit of levitation which means successful levitation was 29% of the nominal rotor mass concerning parameter variation rate in  $H^\infty$  control, it was 73% in the case of  $\mu$  control system.

**2. MODELLING OF FR-MBS**

The dynamics of the flexible-rotor magnetic bearing system will be described in this chapter. For simplicity, the analysis is only done in the  $X$  direction and all the coupling effects among the different axes and noncollocation are ignored. According to the test rig which will be described in Chapter 5, the rotor can be taken simply into account six parts shown in Fig.1.

**2.1 Flexible Rotor Dynamics**

The discrete model with fourteenth-order is obtained using finite element method as follows

$$M_0 \ddot{q} + K_0 q = 0 \tag{1}$$

where  $q = [x_1 \theta_1 \ x_2 \theta_2 \ x_3 \theta_3 \ x_4 \theta_4 \ x_5 \theta_5 \ x_6 \theta_6 \ x_7 \theta_7]^T$  and  $x_i, \theta_i (i=1, \dots, 7)$  represent displacement and angle of the mass on this rotor respectively, especially,  $x_3$  and  $x_5$  represent the positions where the electromagnets are located,  $M_0$  is the mass matrix,  $K_0$  is the stiffness matrix.

**2.2 Actuator Dynamics**

The attractive force due to an electromagnet can be generally given by

$$P = \frac{A}{\mu_0} B^2 = \frac{A}{\mu_0} \left[ \frac{N(i_0 + i)}{1 + \frac{x_0 + x}{\mu}} \right]^2 \tag{2}$$

where  $P$  is the attractive force,  $\mu_0$  is the permeability in the air,  $A$  is the air gap area of one pole,  $B$  is the magnetic flux densities,  $N$  is the number of winding turns,  $i_0$  is the steady-state current,  $x_0$  is the steady-state gap length,  $i$  is the control current,  $x$  is the control gap, and  $\mu$  is the permeability in the magnetic body. Using the Taylor series expansion for small values of  $i$  and  $x$ , we can get the following attractive force with linear terms

$$P \approx p_0 - k_1 x + k_2 i = p_0 + p \tag{3}$$

where

$$k_1 = \frac{2AN^2 i_0^2}{\mu_0^2 \left(\frac{1}{\mu} + \frac{x_0}{\mu_0}\right)^3} = \frac{2p_0}{\mu_0 \left(\frac{1}{\mu} + \frac{x_0}{\mu_0}\right)}$$

$$k_2 = \frac{2AN^2 i_0}{\mu_0 \left(\frac{1}{\mu} + \frac{x_0}{\mu_0}\right)^2} = \frac{2p_0}{i_0}$$

and  $p_0$  is the bias attractive force. Considering the pair of attractive forces, the magnetic force  $P$  due to the electromagnet along the radial direction  $X$  can be modeled as the following equation:

$$\dot{P} = P_1 - P_2 = -2k_1 x + 2k_2 i \tag{4}$$

where  $P_1$  and  $P_2$  are the left and right magnet forces, respectively. Equation(4) indicates that the actuator total forces on each direction.

**2.3 Plant Dynamics**

The flexible rotor shown in Fig.1 is restricted by the attractive forces given in Eq.(4). It results

$$M_0 \ddot{q} + K_0 q = F \dot{p} + D \tag{5}$$

where

$$F = \begin{bmatrix} 0 & 0 & 0 & 0 & 1 & 0 & 0 & 0 & 0 & 0 & 0 & 0 & 0 & 0 \\ 0 & 0 & 0 & 0 & 0 & 0 & 0 & 0 & 1 & 0 & 0 & 0 & 0 & 0 \end{bmatrix}^T$$

$$\dot{p} = [\dot{p}_l \ \dot{p}_r]^T$$

$$P_l = 2k_1 x_3 - 2k_2 i_l : \text{ forces of the AMB-L}$$

$$P_r = 2k_1 x_5 - 2k_2 i_r : \text{ forces of the AMB-R}$$

and  $D$  represents the parameter uncertainty and external disturbance.

The bias attractive forces and the control forces of Eq.(5) are separated as follows:

$$M_0 \ddot{q} + K q = F_i i + D \tag{6}$$

where

$$i = [i_l \ i_r]^T \quad K = K_0 + K_i$$

$$K_i = \text{diag}(0 \ 0 \ 0 \ 0 \ -2k_1 \ 0 \ 0 \ 0 \ -2k_1 \ 0 \ 0 \ 0 \ 0 \ 0)$$

$$F_i = \begin{bmatrix} 0 & 0 & 0 & 0 & -2k_2 & 0 & 0 & 0 & 0 & 0 & 0 & 0 & 0 & 0 \\ 0 & 0 & 0 & 0 & 0 & 0 & 0 & 0 & -2k_2 & 0 & 0 & 0 & 0 & 0 \end{bmatrix}^T$$

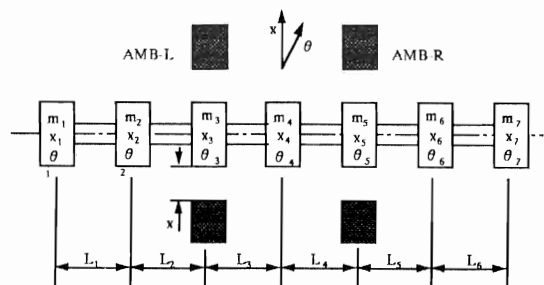


Fig.1 Model of flexible rotor

Using the modal analysis technique, we can choose the following normalized modal matrix,

$$q = \Psi \xi \tag{7}$$

Equation (6) is transformed to the form in model coordinate as follows:

$$\ddot{\xi} + \Lambda \dot{\xi} + \Omega^2 \xi = f_i i + d \tag{8}$$

where

$$I = \Psi^T M \Psi \quad \Omega^2 = \Psi^T K \Psi \quad \Lambda = 2 \zeta \Omega$$

$$f_i = \Psi^T F_i \quad d = \Psi^T D$$

where  $\Lambda$  is called the damping matrix. The damping ratio is determined experimentally. The state equation of the electromagnetic-mechanical system is given by

$$\dot{x}_f = A_f x_f + B_f u + D_f \tag{9}$$

where

$$x_f = \begin{bmatrix} \xi & \dot{\xi} \end{bmatrix}^T \quad u = \begin{bmatrix} i_l & i_r \end{bmatrix}^T$$

$$A_f = \begin{bmatrix} 0 & I \\ -\Omega^2 & -\Lambda \end{bmatrix} \quad B_f = \begin{bmatrix} 0 \\ f_i \end{bmatrix} \quad D_f = \begin{bmatrix} 0 \\ d \end{bmatrix}$$

If the rotor displacement at the magnetic bearings can be measured, the output equation is

$$y = C_f x_f = \begin{bmatrix} x_3 & x_5 \end{bmatrix}^T \tag{10}$$

where

$$C_f = \begin{bmatrix} F_i^T \Psi & 0 \end{bmatrix}$$

### 2.4 Reduced Order Model

Because this MIMO system is originally unstable in open loop, the control objective is to levitate the rotor and maintain the stability. In this case, there are only two unstable rigid modes, and the flexible modes are essentially stable. It is complicated to design a controller including full order models for this high order flexible system. Therefore, the construction of the reduced order model is considered upon the standpoint to stabilize the two rigid modes and to control the vibration of flexible modes. The reduced order model is constructed by truncation of the higher order modes in modal coordinates. Here, the state equation and the output equation including till the *itl* order mode are written as follows:

$$\dot{x}_r = A_r x_r + B_r u + D_r$$

$$y = C_r x_r = \begin{bmatrix} x_3 & x_5 \end{bmatrix}^T \tag{11}$$

where

$$x_r = \begin{bmatrix} \xi_1, \xi_2, \dots, \xi_i, \dot{\xi}_1, \dot{\xi}_2, \dots, \dot{\xi}_i \end{bmatrix}^T$$

Concerning the reduced order model of Eq.(11), the design of control system are done with the case which only the rigid modes are considered. In addition, the closed loop system has to maintain the robust stability without spillover caused by higher order modes ignored above.

### 3. $\mu$ SYNTHESIS THEORY

The block diagram of  $\mu$  synthesis as shown in Fig.2 includes uncertainty in the loop. We call this a generalized component, with a structured uncertainty

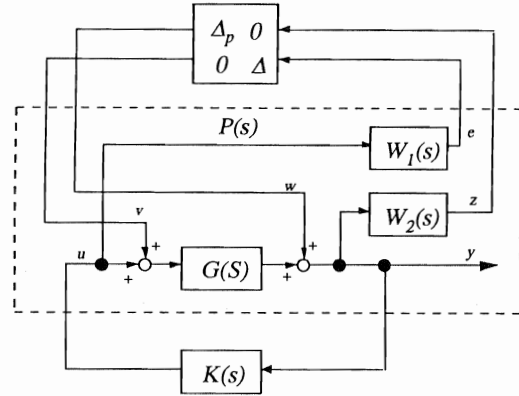


Fig.2 Block diagram of  $\mu$  synthesis

model. In general, the uncertainty matrix is block diagonal, because the uncertainty in a particular component is independent of the uncertainty in other components. The transfer function from  $v$  to  $e$  is

$$\Phi = W_1 K G (I + K G)^{-1} \tag{12}$$

If the following condition

$$\|\Phi\|_{\infty} < 0 \tag{13}$$

is satisfied, it is found that the robust stability condition is accomplished. The transfer function from  $w$  to  $z$  is given by

$$\Phi = W_2 (I + K G)^{-1} \tag{14}$$

So, if the closed loop system satisfy the following condition in any time

$$\|\Phi\|_{\infty} < 1, \tag{15}$$

the nominal performance is achieved. If these two conditions of Eqs.(13) and (15) are simultaneously satisfied, it is just the same as  $H^{\infty}$  control with mixed sensitivity problem. In addition to these conditions, we have to satisfy one more condition in  $\mu$  synthesis as follows;

$$\sup_{\bar{\sigma}(\Delta) \leq 1} \|F_u(M, \Delta)\|_{\infty} \leq 1 \tag{16}$$

where  $F_u$  is call a linear fractional transformation and is defined by

$$F_u(M, \Delta) = M_{22} + M_{21} \Delta (I - M_{11} \Delta)^{-1} M_{12} \tag{17}$$

However, it is so difficult to look for the condition to satisfy Eq.(16). We consider the following expression instead of Eq.(16).

$$\mu_{\Delta}(M) < 1 \tag{18}$$

where,  $\mu_{\Delta}(M) < 1$  is defined by

$$\mu_{\Delta}(M) = \frac{1}{\min\{\bar{\sigma}(\Delta); \Delta \in \Delta, \det(I - M \Delta) = 0\}} \tag{19}$$

$\mu_{\Delta}(M)$  is called a structured singular value. The denominator of Eq.(19) means the smallest perturbation which causes "instability" of the constant matrix feedback loop. As the structured sigular value is converse as shown in Eq.(19), the smaller  $\mu$  means that the limit of destabilization increases for parameter variations and the closed loop system has more strong robust performances. It is known that  $\mu_{\Delta}(M)$  has the following relation,

$$\max \rho(QM) \leq \mu_{\Delta}(M) \leq \inf \bar{\sigma}(DMD^{-1}) \tag{20}$$

where  $D$  is called the scaling matrix. We finally carry

out some computations of  $\inf \bar{\sigma}(DMD^{-1})$  instead of  $\mu_{\Delta}(M)$  for structured singular value.

#### 4. DESIGN OF $\mu$ CONTROL SYSTEM

We designed the  $\mu$  control system using D-K iteration as an approximate solution. The fourth-order system is used for control system design as reduced order model  $G(s)$ . Using the weighting functions  $W_1(s), W_2(s)$  as shown in Fig.3 and the generalized plant  $P(s)$  with the 12th-order as shown in Fig.2, We design the  $H^{\infty}$  controller at first. Next, we did  $\mu$  analysis for the  $H^{\infty}$  controller. Figure 4 shows its  $\mu$  plot. The maximum value of  $\mu$  was 4.6, so it is not enough to satisfy Eq.(18). Therefore, the scaling matrix  $D$  is approximated by a zero-order transfer function with stable and minimum phase. The new generalized plant  $P_2$  is configured including the scaling matrix  $D$ .  $\mu_1$  controller is designed using  $P_2$  and  $\mu$  plot is shown in Fig.5. Since maximum  $\mu$  is 0.82 from Fig.5, the robust performances are accomplished in this system with  $\mu_1$  controller. We had the smallest  $\mu$  plot as shown in Fig.6 in the case of  $\mu_2$  controller in same procedure. Figure 7 shows the designed controllers.

#### 5. EXPERIMENTAL RESULTS

##### 5.1 Test Rig

The test rig of the magnetic bearing system under consideration is shown in Fig.8. The parameter values of this test rig are shown in Table 1. A induction motor rotor is located in the middle of the shaft and two radial magnetic bearings are located on both sides of the motor rotor. A thrust magnetic bearing is located at left end of the shaft. Figure 9 shows the configuration of experiments.

In this experimental set up, a linear analog compensator was also applied in each axis based on the models ignoring the coupling effects among various axes. we can choose the control system by either the linear analog compensator, or  $H^{\infty}, \mu$  control.

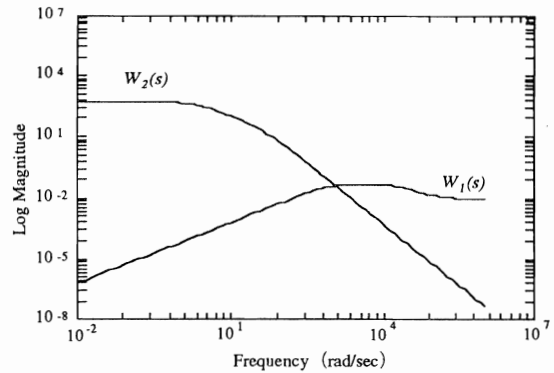


Fig.3 Frequency weighting functions

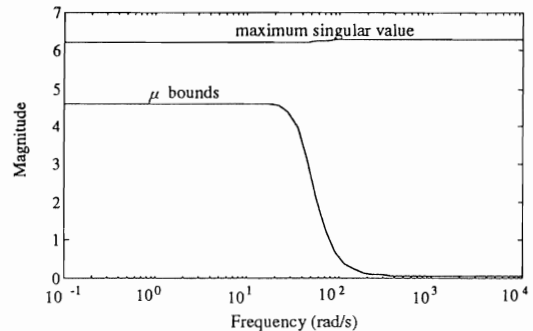


Fig.4 Maximum singular value &  $\mu$  bounds of  $H^{\infty}$  controller

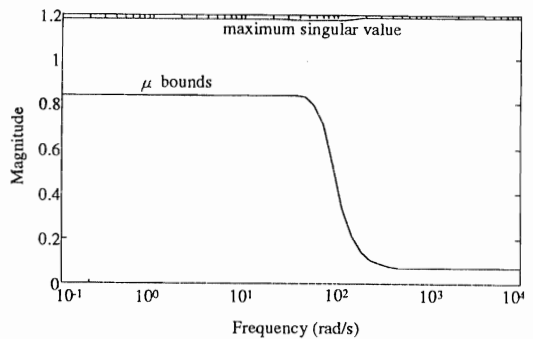


Fig.5 Maximum singular value &  $\mu$  bounds of  $\mu_1$  controller

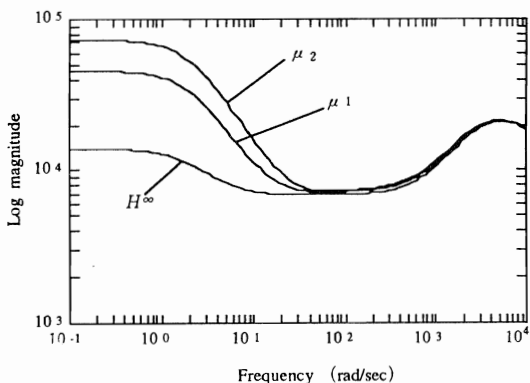


Fig.7 Frequency response of  $H^{\infty}, \mu_1$  and  $\mu_2$  controller

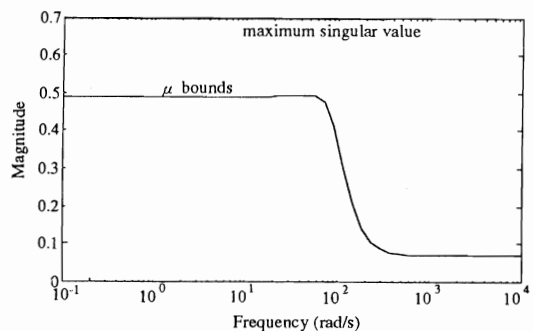


Fig.6 Maximum singular value &  $\mu$  bounds of  $\mu_2$  controller

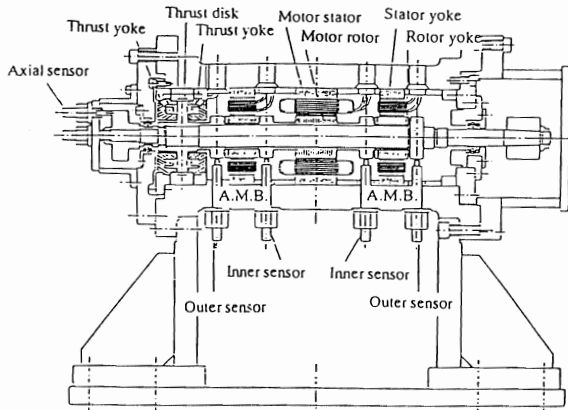


Fig.8 Test rig of flexible rotor magnetic bearing system with five-axis control

### 5.2 $\mu$ Control with Two-Axis Control

In this section, the  $x$  direction is controlled by  $H^\infty$  and  $\mu$  control, and the  $y$  direction is by PID control. Figures 10(a), 11(a) and 12(a) show the typical step time history response at the lift off. It is found that the offset is reduced in the case of  $\mu_2$  controller. This is caused by the strong integrator. Figures 10(b), 11(b) and 12(b) show the robust performances for parameter variations in cases that the rotor mass increases. The nominal mass of the rotor is 5.5 Kg. The upper limits of variation rates from the nominal value are 15% for  $H^\infty$ , 40% for  $\mu_1$  and 50% for  $\mu_2$ . This means that the system becomes unstable if the perturbation exceeds these rates. It can be seen that the closed loop system with  $\mu_2$  controller has superior robust performances to eliminate disturbances and to maintain the low sensitivity for the system parameter variation. It is very important to decrease the structured singular value  $\mu$  if possible. It is not easy for conventional analog compensator to realize the similar good performance.

### 5.3 $\mu$ Control with Four-Axis Control

Next, both of the  $X$  and  $Y$  directions are controlled by DSP based  $H^\infty$  and  $\mu$  control. Figures 13, 14 and 15 show the step time history responses at the lift off. In these cases, the robust performances go up comparing with Section 5.2. The upper limits of variation rates from the nominal value are 29% for  $H^\infty$ , 56% for  $\mu_1$  and 73% for  $\mu_2$ . It is considered that the upper limits of variation rate go down because PID controller cannot realize excellent robust performances in the case of Section 5.2. These results are very similar to the simulation results. We have already succeeded high speed rotating tests up to 30000 rpm using  $\mu_2$  controller.

## 6. CONCLUSIONS

In this paper, we designed  $\mu$  controllers for flexible rotor /magnetic bearing systems applying  $\mu$  synthesis theory.

Table 1 Parameters used for modelling

Parameter	Value	Parameter	Value
Mass $m_1$	0.03 kg	Diameter $d$	0.0275 m
$m_2$	0.15 kg	Gap $x_0$	0.0003 m
$m_3$	1.0 kg	Bias current $i_0$	3.0 A
$m_4$	0.5 kg	Bias attractive force $p_b$	100.0 N
$m_5$	1.0 kg	Damping ratio ( $j=1, \dots, 14$ ) $\xi_j$	0.001
$m_6$	0.0 kg	Permeability in magnetic body $\mu$	$2\pi \times 10^{-3}$
$m_7$	0.09 kg	Permeability in magnetic air $\mu_0$	$4\pi \times 10^{-7}$
Length $L_1$	0.09 m		
$L_2$	0.072 m		
$L_3$	0.09 m		
$L_4$	0.09 m		
$L_5$	0.091 m		
$L_6$	0.091 m		

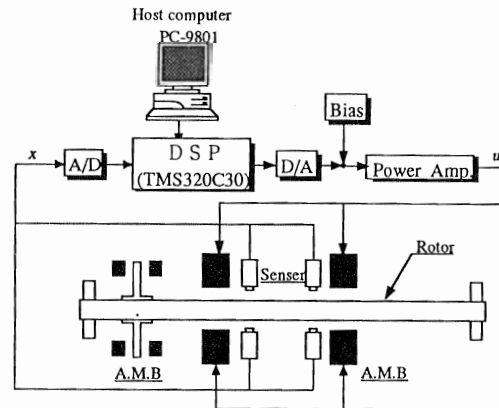


Fig.9 Configuration of DSP-based  $\mu$  control system

The excellent robust performances of  $\mu$  control system are made clear comparing with  $H^\infty$  control. The conclusions are summarized as follows;

- (1) We have realized the stabilization of the magnetic levitation system with high stiffness applying  $\mu$  synthesis theory.
- (2) It is found that  $\mu$  control system has excellent robust performances comparing with  $H^\infty$  control through simulations and experiments.
- (3) It is very important to decrease the structured singular value  $\mu$  to realize a excellent robust performance.

## ACKNOWLEDGMENTS

The authors gratefully acknowledge the support of Ebara Research Co., Ltd. of Japan for the experimental set up.

## REFERENCES

- [1] Cui W. and Nonami K.,  $H^\infty$  Control of Flexible Rotor-Magnetic Bearing Systems, Proc. of the 3rd Int. Sym. on Magnetic Bearings, 505-512, 1992.
- [2] Nonami K. and Fan Q., Computer-Aided Control System Design and Control Performance for Active Vibration Control with  $\mu$  Synthesis Theory,

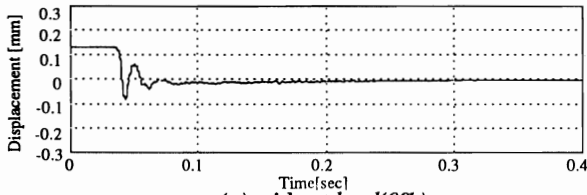
Transactions of JSME (in Japanese), C, 60-572, 1203-1209, 1994.

[3] Nonami K. and Tian H.: Sliding Mode Control, Corona Pub., (in Japanese), 1994.

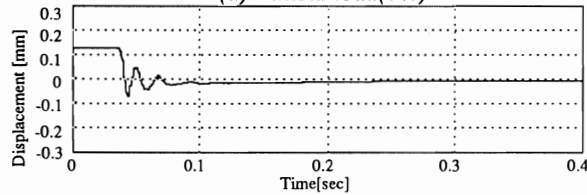
[4] Doyle J., Analysis of Feedback Systems with

Structured Uncertainty, IEEE Proc., Part D, 129, 242-250, 1982.

[5] Balas G., Doyle J., Glover K., Packard A. and Smith R.,  $\mu$  Analysis and Synthesis Toolbox User's Guide, Musysn Inc., 1991.

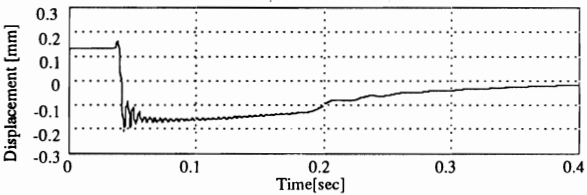


(a) without load(0%)

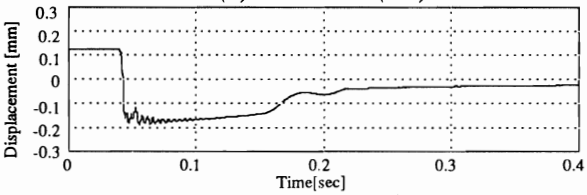


(b) with load of 0.8 Kg(15%)

Fig.10 Step response in levitation for parameter variations ( $H$  controller) with two-axis control

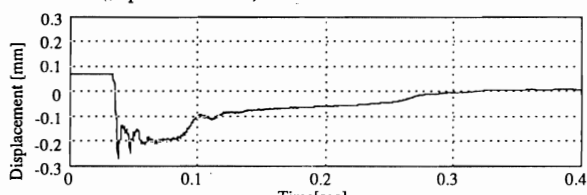


(a) without load(0%)

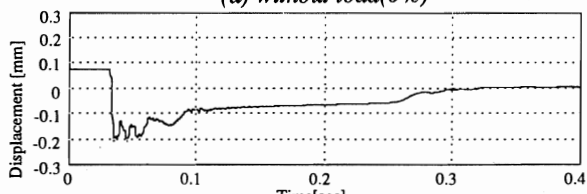


(b) with load of 2.2Kg(40%)

Fig.11 Step response in levitation for parameter variations ( $\mu_1$  controller) with two-axis control

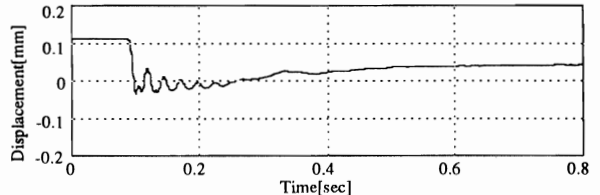


(a) without load(0%)

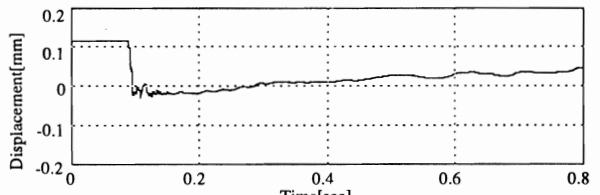


(b) with load of 2.5Kg(45%)

Fig.12 Step response in levitation for parameter variations ( $\mu_2$  controller) with two-axis control

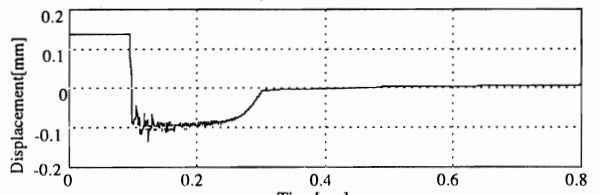


(a) without load(0%)

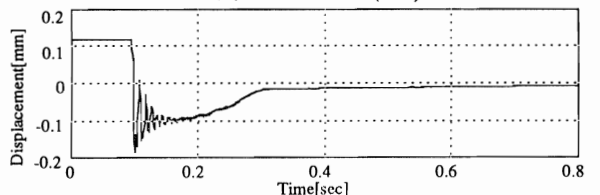


(b) with load of 1.58Kg(29%)

Fig.13 Step response in levitation for parameter variations ( $H$  controller) with four-axis control

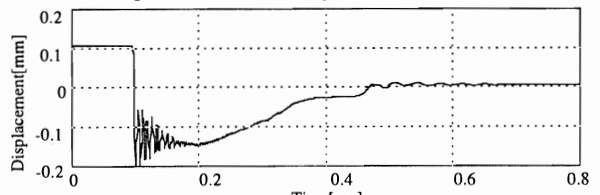


(a) without load(0%)

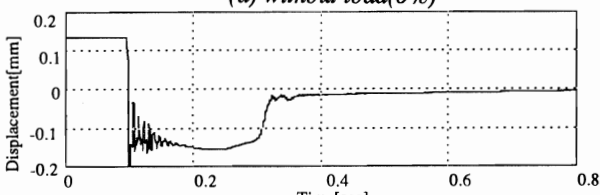


(b) with load of 3.1Kg(56%)

Fig.14 Step response in levitation for parameter variations ( $\mu_1$  controller) with four-axis control



(a) without load(0%)



(b) with load of 4.0Kg(73%)

Fig.15 Step response in levitation for parameter variations ( $\mu_2$  controller) with four-axis control